

Designing the Safe Reopening of US Towns Through High-Resolution Agent-Based Modeling

Original

Designing the Safe Reopening of US Towns Through High-Resolution Agent-Based Modeling / Truszkowska, A., Thakore, M., Zino, L., Butail, S., Caroppo, E., Jiang, Z.-P., Rizzo, A., Porfiri, M.. - In: ADVANCED THEORY AND SIMULATIONS. - ISSN 2513-0390. - ELETTRONICO. - 4:9(2021), p. 2100157. [10.1002/adts.202100157]

Availability:

This version is available at: 11583/2957664 since: 2022-03-08T16:48:44Z

Publisher:

John Wiley and Sons Inc

Published

DOI:10.1002/adts.202100157

Terms of use:

This article is made available under terms and conditions as specified in the corresponding bibliographic description in the repository

Publisher copyright

Wiley postprint/Author's Accepted Manuscript

This is the peer reviewed version of the above quoted article, which has been published in final form at <http://dx.doi.org/10.1002/adts.202100157>. This article may be used for non-commercial purposes in accordance with Wiley Terms and Conditions for Use of Self-Archived Versions.

(Article begins on next page)

1 Designing the safe reopening of US towns through high- 2 resolution agent-based modeling

3 *Agnieszka Truszkowska, Malav Thakore, Lorenzo Zino, Sachit Butail, Emanuele Caroppo,*
4 *Zhong-Ping Jiang, Alessandro Rizzo, and Maurizio Porfiri**

5 Dr. A. Truszkowska

6 Center for Urban Science and Progress, Tandon School of Engineering, New York Univer-
7 sity, 370 Jay Street, Brooklyn, NY 11201, USA

8 Department of Mechanical and Aerospace Engineering, Tandon School of Engineering, New
9 York University, Six MetroTech Center, Brooklyn NY 11201, USA

10 Malav Thakore, Prof. S. Butail

11 Department of Mechanical Engineering, Northern Illinois University, DeKalb IL 60115,
12 USA

13 Dr. L. Zino

14 Faculty of Science and Engineering, University of Groningen, Nijenborgh 4, 9747 AG Gronin-
15 gen, The Netherlands

16 Prof. E. Caroppo

17 Department of Mental Health, Local Health Unit ROMA 2, 00159 Rome, Italy

18 University Research Center He.R.A., Università Cattolica del Sacro Cuore, 00168 Rome,
19 Italy

20 Prof. Z.-P. Jiang

21 Department of Electrical and Computer Engineering, Tandon School of Engineering, New
22 York University, 370 Jay Street, Brooklyn NY 11201, USA

23 Prof. A. Rizzo

24 Department of Electronics and Communications, Politecnico di Torino, 10129 Turin, Italy
25 Office of Innovation, Tandon School of Engineering, New York University, Six MetroTech
26 Center, Brooklyn NY 11201, USA

27 Prof. M. Porfiri

28 Center for Urban Science and Progress, Tandon School of Engineering, New York Univer-
29 sity, 370 Jay Street, Brooklyn, NY 11201, USA

30 Department of Mechanical and Aerospace Engineering, Tandon School of Engineering,
31 New York University, Six MetroTech Center, Brooklyn NY 11201, USA

32 Department of Biomedical Engineering, Tandon School of Engineering, New York Univer-
33 sity, Six MetroTech Center, Brooklyn NY 11201, USA

34 Email Address: mporfiri@nyu.edu

35 Keywords: *agent-based model, COVID-19, epidemiology, urban science, vaccination*

36 As COVID-19 vaccine is being rolled-out in the US, public health authorities are gradually reopening the economy.
37 To date, there is no consensus on a common approach among local authorities. Here, a high-resolution agent-based
38 model is proposed to examine the interplay between the increased immunity afforded by the vaccine roll-out and
39 the transmission risks associated with reopening efforts. The model faithfully reproduces the demographics, spa-
40 tial layout, and mobility patterns of the town of New Rochelle, NY — representative of the urban fabric of the US.
41 Model predictions warrant caution in the reopening under the current rate at which people are being vaccinated,
42 whereby increasing access to social gathering in leisure location and households at a 1% daily rate can lead to 28%
43 increase in the fatality rate within the next three months. The vaccine roll-out plays a crucial role on the safety of
44 reopening: doubling the current vaccination rate is predicted to be sufficient for safe, rapid reopening.

45 1 Introduction

46 One year after the global outbreak of COVID-19, the World is finally witnessing the roll-
47 out of vaccination campaigns. As more and more people are becoming immune to the dis-
48 ease, policy makers are gradually devising the uplifting of restrictive policies. With over
49 2.4% of the World and almost 24% of the US population fully vaccinated as of mid-April
50 2021, ^[1] governments are increasingly seeking to resume normal activities in all segments of
51 life. Many US states are actively reopening all their non-essential services and reducing the
52 strictness of some of their public health measures. The epidemiological effects of these re-
53 opening efforts are still under debate, with diverging opinions across political aisles and too
54 few empirical observations to draw statistically-grounded claims. ^[2–4] While it is generally
55 accepted that the ongoing vaccine roll-out will gradually reduce the spread, the extent to
56 which it can afford safe reopening of the economy remains elusive. There is a pressing need
57 for scientifically-backed approaches that can inform policy-making to relaunch the economy
58 and resume normalcy, without resurgent COVID-19 waves.

59 Since the inception of the worldwide COVID-19 pandemic in January 2020, mathemati-
60 cal models have emerged as powerful tools to combat the spread. ^[5–7] In the first phase of
61 the pandemic, models have been largely used to conduct what-if analyses on the effect of
62 nonpharmaceutical interventions (NPIs) for the containment of the spread, ^[8–12] also con-
63 sidering their socio-economic and mental impact. ^[13–15] More recently, models are gain-
64 ing use as decision support systems to design efficient vaccination campaigns. ^[16–24] Ef-
65 fective vaccine roll-out strategies are the solution of complex optimization problems, due
66 to limited availability of vaccines, differential effectiveness and adverse effects across age
67 strata and fragility profiles, time constraints on double-dose administration, and distribu-
68 tion issues. ^[16,17] Ongoing efforts have quantitatively addressed several aspects of vacci-
69 nation campaigns. In Shen *et al.*, ^[18] the admissible level of relaxation of NPIs has been
70 evaluated as function of vaccination coverage and effectiveness of the vaccine. Giordano
71 *et al.* ^[19] and Moore *et al.* ^[20] have highlighted the importance of maintaining NPIs during
72 early stages of the vaccination in Italy and the United Kingdom, respectively. The prob-
73 lem of coordinating the early-stage vaccination campaign and intervention policies has also
74 been investigated in other studies, ^[21–24] focusing on the spread of virus variants that are
75 potentially resistant to the vaccine.

76 Overall, these modeling efforts provide important insight into several aspects of vaccine
77 roll-outs, but they are based on coarse-grained assumptions that may not capture the com-
78 plexity of the spreading dynamics. Whether they employ compartments ^[18,19,21,23,24] or
79 meta-populations, ^[20,22] these models cannot resolve the richness of the geographical distri-
80 bution of the population, the different epidemiological risk factors associated with the loca-

81 tions where people can come into contact, and the wide range of mobility patterns, among
82 other factors. Agent-based models (ABMs) represent a powerful alternative to compart-
83 mental and meta-population models, one that is able to describe spreading dynamics with
84 the accuracy and detail that is needed to support the assessment of different intervention
85 strategies. [25–27] In particular, through ABMs, it is possible to accurately simulate COVID-
86 19 spread over entire towns. [28]

87 Here, we propose a high-resolution ABM of a medium-sized US town (New Rochelle, NY),
88 for which we systematically examine the interplay between the risks associated with re-
89 opening efforts and the increased immunity afforded by the vaccine roll-out. We specifi-
90 cally seek to understand what should be the speed of the vaccination campaign that will
91 afford safe reopening of the economy. The model operates at a full population resolution,
92 so that one agent in the model corresponds to one individual within the population of New
93 Rochelle. Using publicly available data, the model faithfully reproduces the town demo-
94 graphics, the spatial layout and use of every town building, and the mobility patterns of
95 the entire population.

96 2 Results

97 2.1 High-resolution COVID-19 ABM with human mobility

98 Our computational framework consisted of two elements: a database of a US town and a
99 highly granular agent-based model (ABM) of COVID-19 with human mobility. The database
100 reproduced the town of New Rochelle, NY, where one of the first US COVID-19 outbreaks
101 took place. [29] New Rochelle has a population of 79,205 [30] and a representative structure
102 of many urban areas in the US. [31] The population was recreated using US Census statistics, [30]
103 accounting for realistic age distribution, household and family structure, and occupational
104 characteristics of the town’s residents. US Census data [30] was also used for the assignment
105 of workplaces for the agents, encompassing work from home, in the town, or in nearby lo-
106 cations (including the New York City boroughs, upstate New York, and Connecticut). Uti-
107 lizing data from OpenStreetMap, [32] Google Maps, [33] and Safegraph, [34] we assembled a
108 database including every building in the town, residential or public, see Methods Section.

109 The proposed ABM is a highly granular model that simulated COVID-19 spread to afford
110 “what-if” analyses on public health measures, whose backbone was first introduced in our
111 previous work. [28] Every individual in the town is represented as an agent, and the spread
112 of COVID-19 is modeled by explicitly considering their households, lifestyles, schools, and
113 workplaces. The model incorporates known stages of the COVID-19 disease progression,
114 that is, the pre-symptomatic, the symptomatic phase, and the possibility of never devel-
115 oping symptoms. The two possible outcomes of the disease, recovery and death, are in-
116 cluded in the ABM. Over the duration of the disease, the agents can be tested for COVID-
117 19, quarantined, hospitalized, and treated in an intensive care unit. The model can also
118 simulate vaccination campaigns and a wide variety of NPIs, including school closures, lock-
119 downs, and social distancing, and, indirectly, the use of PPE.

120 Toward examining the role of reopening efforts on COVID-19 spread, we extended our pre-
121 vious effort [28] to include realistic human mobility patterns; the new components are sum-
122 marized in Figure 1, see Methods Section. Specifically, the improved framework incorpo-
123 rates the following mobility patterns: i) agents can work outside the town; ii) agents can

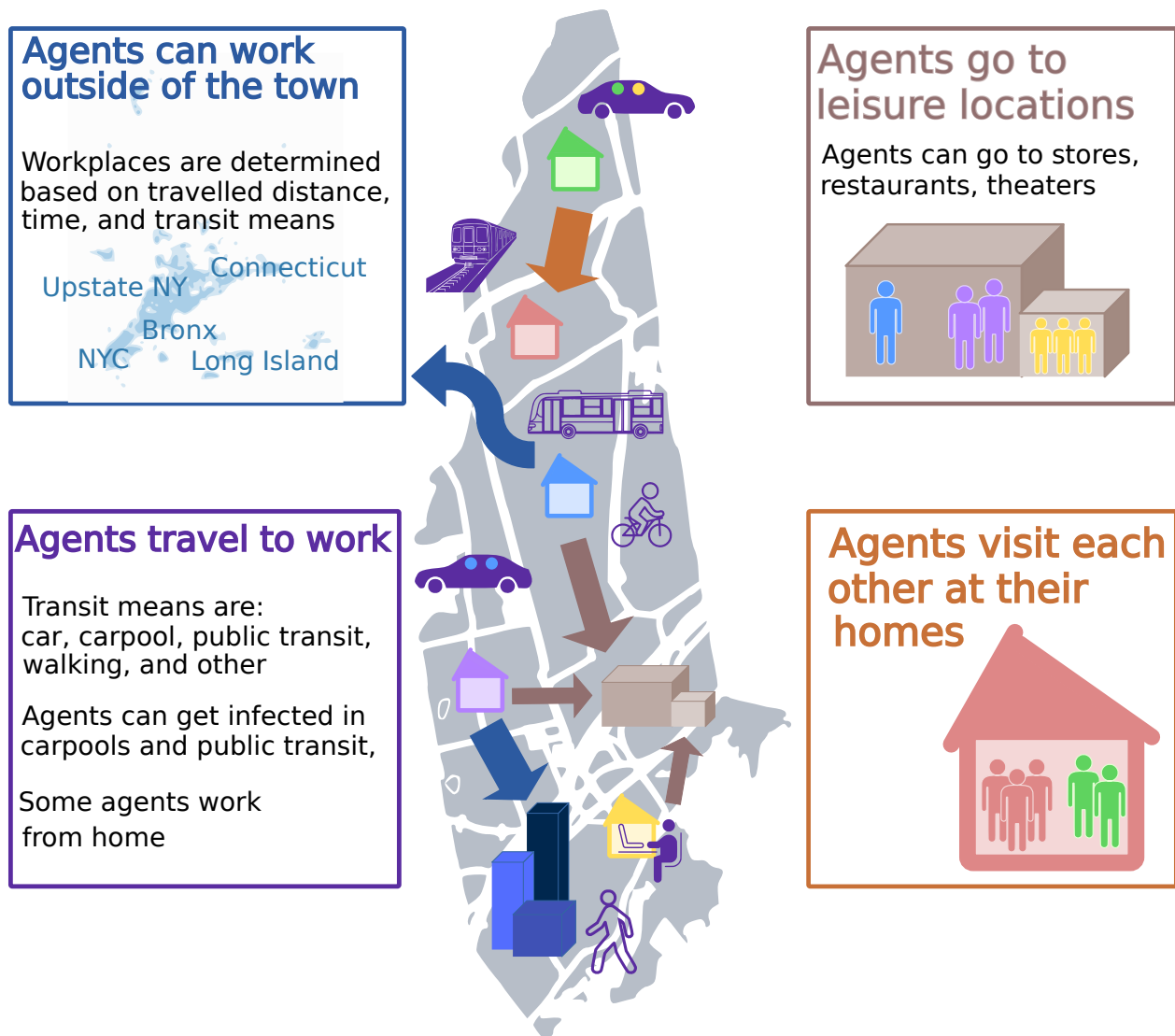


Figure 1: Schematic outline of the model and human mobility elements. The model simulates all the residents of New Rochelle, NY. In addition to residences, hospitals, workplaces, and schools, COVID-19 can spread during transit, in leisure locations, and when socializing in private. A portion of the population works outside of town, in nearby areas that are also experiencing COVID-19 spreading.

124 travel to work through five different modes of transportation; iii) agents can spend time in
125 leisure locations, such as cinemas, theaters, and restaurants; and iv) agents can visit each
126 other to socialize. Agents travel to work via five transit modes identified in the US Cen-
127 sus: car, carpool, public transit, walking, and others, such as cycling. COVID-19 spread
128 was only modeled in carpools and public transit.

129 We conducted a series of simulations to assess the interplay between the vaccine roll-out
130 and the reopening of the economy on the spread of COVID-19. The spread of COVID-19
131 was simulated by initializing the ABM with officially reported, county-level statistics, in-
132 cluding those on the number of undetected and asymptomatic cases (in total 187 active
133 cases). The vaccine roll-out was modeled as a constant fraction of the town population be-
134 ing immunized each day. Reopening efforts were modeled by increasing the frequency at
135 which agents visited leisure locations and each other (see Methods). To quantify the me-
136 diating role of testing, we performed these simulations at three different efficacies: i) aver-
137 age testing as calibrated in our previous work [28] for the Spring and early Summer of 2020
138 (64% of the symptomatic and 44% of the asymptomatic are detected); ii) perfect testing,
139 where all but those who were asymptomatic at the beginning of the simulations undergo
140 testing; and iii) intermediate testing, between i) and ii) (82% of the symptomatic and 72%
141 of the asymptomatic are detected). Across all levels, we included a 95% confidence in the
142 test accuracy, thereby leading to false negatives even for perfect testing.

143 2.2 Current vaccination rates warrant caution in reopening efforts

144 When simulated for three months with a recent vaccination rate of 0.57% population/day, [1]
145 Figure 2 reveals a clear influence of the reopening rate on the number of infections across
146 all levels of testing efficacies. In all scenarios, the total number of infected visibly increases
147 with the reopening rate, eventually plateauing to a maximum value.

148 In particular, as reopening rates exceed 0.1%/day, the total number of infected rises re-
149 gardless of the efficacy of testing. To put this claim in context, from SafeGraph data, [34]
150 we estimated the present reopening rate in NY to be approximately 0.28%/day, see Meth-
151 ods Section. As the reopening rates increase beyond about 3%/day, the number of infected
152 levels out to a maximum value. With respect to the number of deaths, we registered a sim-
153 ilar trend of a steep initial rise followed by a plateau for both low and moderate tracing;
154 for perfect tracing, the number of deaths has a marginal dependence on the reopening rate.

155
156 As expected, the testing efficacy itself has a critical effect on the number of infections and
157 deaths with an approximately tenfold increase in each value as efficacy goes from perfect
158 to low. More worryingly, however, for low testing and the current vaccination rate, we ob-
159 served a 28% increase in fatality rate as the reopening rate rises by only 1%/day.

160 2.3 Faster, yet safe reopening is possible with more daily vaccinations

161 To quantify the extent to which faster vaccine roll-out can mitigate the adverse epidemio-
162 logical effects of reopening, we performed a second, more extensive, study. Specifically, we
163 compared the cumulative number of infections and the death toll for a range of possible
164 vaccination and reopening rates. Results, shown in Figure 3, indicate that, while aggres-
165 sive vaccination campaigns can offset ambitious reopening efforts, low vaccination rates can

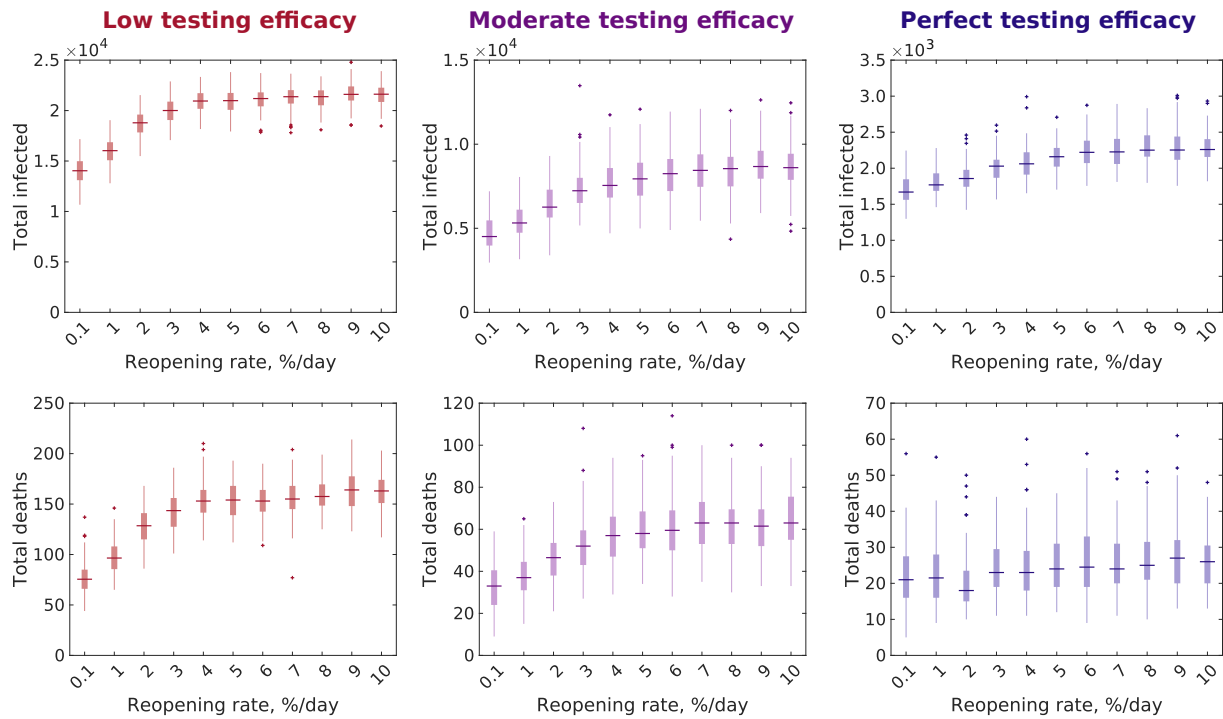


Figure 2: Impact of the reopening rate on the spread of COVID-19 over a three-month duration. The three different testing efficacies—low, moderate, and perfect—correspond to different detection levels across asymptomatic and symptomatic individuals. Note that the maximum value along the ordinate is different for each level of testing. The bottom and top edges of the box plots mark the 25th and 75th percentiles, the solid lines represent the median, and the whiskers span entire, outlier-free dataset; outliers are denoted by ‘+’ symbols.

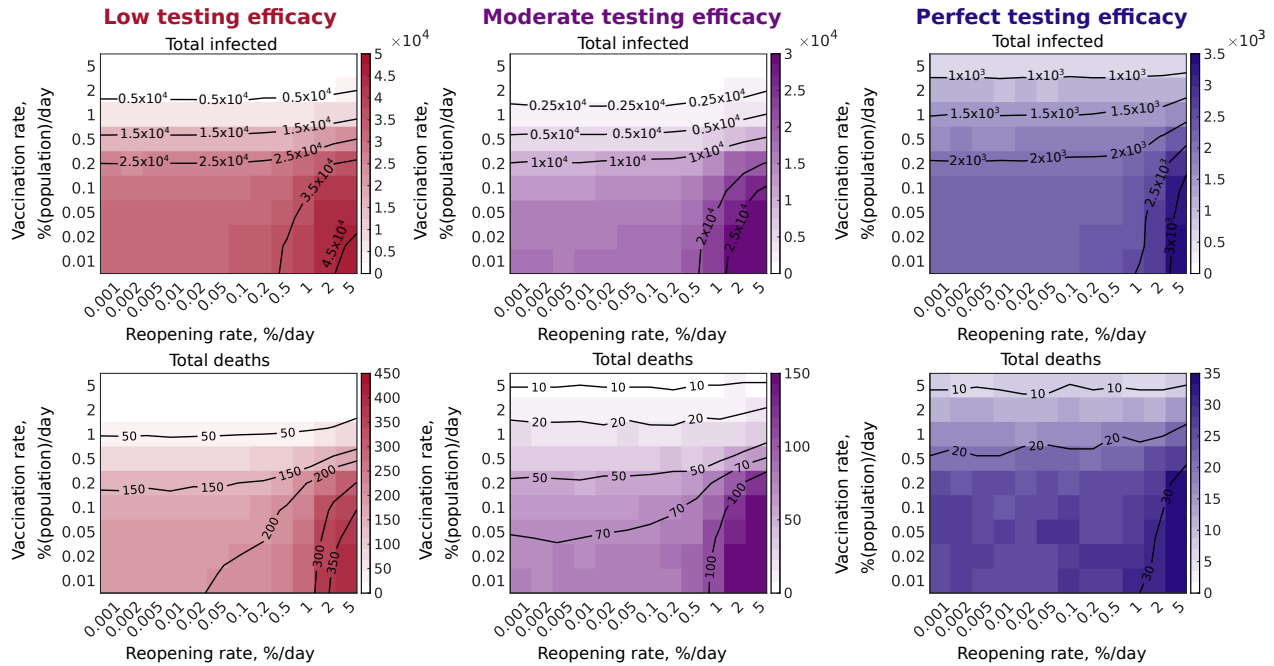


Figure 3: Interplay between vaccine roll-out and reopening rates, in the form of two-dimensional heatmaps. The colorbar on the right of each heatmap shows the total number of infected and deaths are reported as a function of varying vaccination and reopening rates. Contour lines are also plotted for clarity.

166 easily degenerate into dramatic growths in number of infections and fatalities as reopening
 167 rates increase.

168 Specifically, we found that: a) high vaccination rates, above 1% population/day, can bring
 169 down infections and fatalities dramatically to less than 10, at even the fastest reopening
 170 rate of 5%/day; b) the reopening rate has a secondary effect on the numbers of infections
 171 and deaths when vaccination rates exceed 0.2%, as evidenced by near horizontal contour
 172 lines within that region of the heatmaps; and c) high reopening rates, above 1%/day, can
 173 lead to a dramatic increase in the numbers of infections and deaths if not supported by ag-
 174 gressive vaccination campaign. Overall, these plots point at a rich, nonlinear interplay be-
 175 tween vaccination and reopening rates on COVID-19 spread, upon which we recommend
 176 doubling the current rate of vaccination to at least 1%/day to afford safe reopening.

177 Comparing across different levels of testing, we noted, once again, the crucial role that ef-
 178 ficacious testing plays in containing the number of infections and deaths. In particular,
 179 while the general implications of high vaccination rates and low reopening rates remain the
 180 same, the actual numbers scale down by a factor of ten as the efficacy of testing drops from
 181 perfect to low, confirming the critical role of capillary and continuous testing of the popu-
 182 lation.

183 3 Discussion and conclusion

184 In this work, we examined the complex interplay between the transmission risks brought
 185 about by ongoing reopening efforts and increased immunity offered by vaccine roll-out on
 186 the spread of COVID-19 in an urban setting. We designed and implemented a highly gran-

187 ular ABM, by extending the effort of Truskowska *et al.* [28] to account for population mo-
188 bility, non-essential leisure activities and gatherings in households, progressive reopening
189 efforts, and vaccination campaigns. The model was calibrated on New Rochelle, NY, a medium-
190 sized town representative of a vast class of US urban areas. We explored both current and
191 hypothetical vaccination campaigns, for three realistic scenarios of testing efficacy.

192 Our results indicate that today’s vaccination rate of 0.57% population/day [1] in New Rochelle,
193 NY, can only support a careful reopening. With the current vaccine roll-out, reopening ef-
194 forts would always lead to a rise in the numbers of infected individuals and casualties; not
195 even under a perfect testing where every infected individual is traced and isolated, it would
196 be possible to halt COVID-19 spread. The present reopening rate of 0.28%/day could lead
197 to a number of deaths as high as one hundred and fifty, a mortality rate similar to the “first
198 wave”. These findings are in agreement with other studies that have shown that the relax-
199 ation of NPIs always causes increases of COVID-19 infections and deaths. Shen *et al.* [18]
200 established that under current levels of vaccine effectiveness and coverage in the US, mod-
201 erate NPIs, in the form of partial use of PPEs, are required to prevent further outbreaks.
202 Likewise, Giordano *et al.* [19] demonstrated that the current vaccine roll-out in Italy does
203 not support uplifting of NPIs, without a substantial rise of infections and casualties. Many
204 other research efforts have confirmed that rapid lifting of NPIs would have dramatic con-
205 sequences on the spread of COVID-19, notwithstanding the current vaccine roll-out. [20–24]
206 In general, the scientific community has reached consensus on the need of extreme caution
207 in reopening the economy, in support to concerns of about half of the US population who
208 fear that the current status of the vaccination campaign may not be conducive to return to
209 normalcy in the near future. [2]

210 We then conducted a what-if analysis for different vaccination rates, toward determining
211 whether safe reopening could be supported by a faster vaccine roll-out than the current
212 one. We registered the existence of a trade-off between the vaccination and reopening rates
213 with respect to the numbers of infections and casualties. While for low vaccination rates
214 we observed a dramatic growth in infection and death counts as the reopening rate increases,
215 cases and deaths settle around constant values for sufficiently high vaccination rates. Our
216 findings suggest that doubling the current vaccination rate to at least 1% population/day
217 could support safe and fast comeback to normalcy, whereby reopening could be accelerated
218 without sensibly affecting COVID-19 spread. It is tenable that this phenomenon is related
219 to the reduction of the effective reproduction number in response to vaccine roll-out above
220 a critical rate, which has been observed in simplified compartmental models. [35]

221 Lastly, our study echoes experts in highlighting the importance of efficacious testing for
222 safe reopening, even in the current phase of the pandemic when mass vaccination is ongoing. [36,37]
223 The United Kingdom, for example, is offering free testing to each person twice a week, start-
224 ing from April 9, 2021. [38] Specifically, we assessed the implications of three increasingly
225 efficacious testing scenarios, from the lowest one corresponding to the first wave (Summer
226 2020) and the best one to ideal conditions. While the trends regarding the interplay be-
227 tween vaccination and reopening rates do not qualitatively change with testing, the sheer
228 toll of the epidemic increases dramatically for low levels of testing efficacy. Notably, we
229 registered that perfect testing may reduce casualties by one order of magnitude with re-
230 spect to the worst-case scenario, for most of the combinations of vaccination and reopening
231 rates.

232 Our findings are consistent with claims drawn by other studies in the literature, ^[18–24] which
233 warrant caution in reopening the economy on the basis of current vaccination rates. How-
234 ever, the cited studies are based on lumped age-structured compartmental or metapopu-
235 lation models that can hardly capture the complexity and spatial structure of urban envi-
236 ronments, along with details about behavioral traits of the population at the granularity of
237 the single individual. Coarse-grained models smear the details that are captured by ABMs
238 into a few macroscopic parameters, from which it is difficult to draw actionable decisions to
239 steer interventions in the field.

240 When interpreting the results of our study, one needs to acknowledge several limitations
241 of the model, the major one due to the resolution and quality of the available data — a
242 common issue in the literature. For example, initial conditions on the health state of the
243 town population are not directly available and were calibrated by rescaling available data
244 at the county level. Likewise, the baseline values for the visits to leisure locations and pri-
245 vate households prior to the reopening are educated guesses, based on publicly available
246 local mobility data. Along with data limitations, we should acknowledge a range of simpli-
247 fying assumptions that, within the philosophy of ABMs [39], are needed to reconcile com-
248 putational complexity and model granularity with respect to public transport routes within
249 the town, behavioral traits of the individuals, boundary conditions of the model, reopen-
250 ing efforts, and vaccine roll-out. For example, we set a uniform global parameter quanti-
251 fying the reopening rate for all non-essential venues (leisure and house gatherings), with-
252 out resolving one business versus another. Likewise, we assumed that vaccines have ideal
253 efficacy, whereby a vaccinated agent becomes fully immune to COVID-19. This likely opti-
254 mistic choice was dictated by the present uncertainty on the vaccine efficiency, also in light
255 of new virus strains that are still under investigation. Lastly, we did not explicitly model
256 contact tracing, although our ABM could be extended to faithfully reproduce real-world
257 contact tracing practices, similar to those implemented by Reyna-Lara et al. ^[40] and Ko-
258 jaku et al. ^[41]

259 As more people get vaccinated across the world, there is an understandable urge to reopen
260 the economy. With arguments both in favor of and against accelerated return to normalcy
261 reaching a high media pitch, it is critical that such debates be informed by scientifically
262 grounded evidence. Our ABM offers a detailed representation of a mid-sized US town at
263 the level of a single individual, which can support policy makers in assessing the cost/benefit
264 ratios of reopening. The model is open source and accessible to researchers and practition-
265 ers across the World.

266 4 Methods

267 Our modeling framework consisted of two elements. The first was a detailed database of a
268 US town, including its demographics, buildings and gathering locations, and mobility pat-
269 terns of the population. The second was an ABM that emulates human mobility and be-
270 havior in the town, along with a location-specific epidemic transmission and progression
271 model tailored to COVID-19. The model contemplated testing, isolation, treatment, and
272 vaccination. In the following, we detail the salient features of all the model components.

4.1 Database

The spatial layout of New Rochelle, NY was mapped by recording geographic coordinates and occupancy information of relevant locations, such as households, in-town and out-of-town workplaces, schools, retirement homes, hospitals, and leisure locations. Locations and capacities of in-town residential and public buildings, including schools, retirement homes, and the local hospital, were collected using OpenStreetMap^[32] and Google Maps.^[33] The locations and capacities of out-of-town workplaces and in-town leisure venues were gathered using SafeGraph;^[34] leisure locations included a variety of stores, restaurants, arts, sports, and entertainment venues visited as part of a regular, off-work activity, see the Supporting Information for further details.

The synthetic ABM population comprised 79,205 agents and was generated to statistically match the age distribution from the most recent US Census data.^[30] We exactly matched the number of agents assigned to households and residential buildings, and the number of residents in the retirement homes was estimated based on the size of such facilities. Students were assigned to schools using data from the National Center of Education Statistics.^[42] The process of assigning agents to workplaces was informed by US Census data^[30] about modes of transportation to work and travel times. Specifically, we estimated the distances from agents' households to their workplaces using US Census statistics on traveling times and transit modes. We then statistically assigned agents to workplaces in or outside of the town by matching the distributions of such distances and of the number of employees within each workplace. At the onset of the simulation, the number of hospital patients was determined using data from the New York State Department of Health^[43] and the American Hospital Directory.^[44]

4.2 COVID-19 progression model

At each time-step, each agent could interact with other agents in the different locations they are assigned to (households, workplaces, schools, retirement homes, public transit, carpools, non-essential activities, and hospital). Agents could be susceptible to the disease, undergoing testing, under treatment, or vaccinated. We also assumed that new agents do not enter during the simulation.

The progression model comprised six main states: susceptible (S), exposed—including asymptomatic individuals—(E), symptomatic (Sy), vaccinated (V), removed-healthy/recovered (R), and removed-dead (D). A detailed progression graph is illustrated in Figure 4. The exposed (E) state was attained by agents upon infection. When a latency period was over, exposed agents might develop symptoms and become symptomatic (Sy). Symptomatic individuals were prevented from going to school and work, but they could freely move on public transportation and go to leisure locations or private households, for example to get basic necessities. Some exposed agents might recover without ever developing symptoms and transition to R .

Vaccinated agents (V) were assumed to be immune to COVID-19. At each time-step Δt , a constant fraction of the population ν , termed vaccination rate, randomly drawn from the susceptible agents (S) was vaccinated. These agents transitioned to state V . Susceptible, exposed, and symptomatic agents could undergo testing in a hospital (T_{Hs}) — carrying the possibility of infecting hospital staff and patients, or being infected if susceptible — or

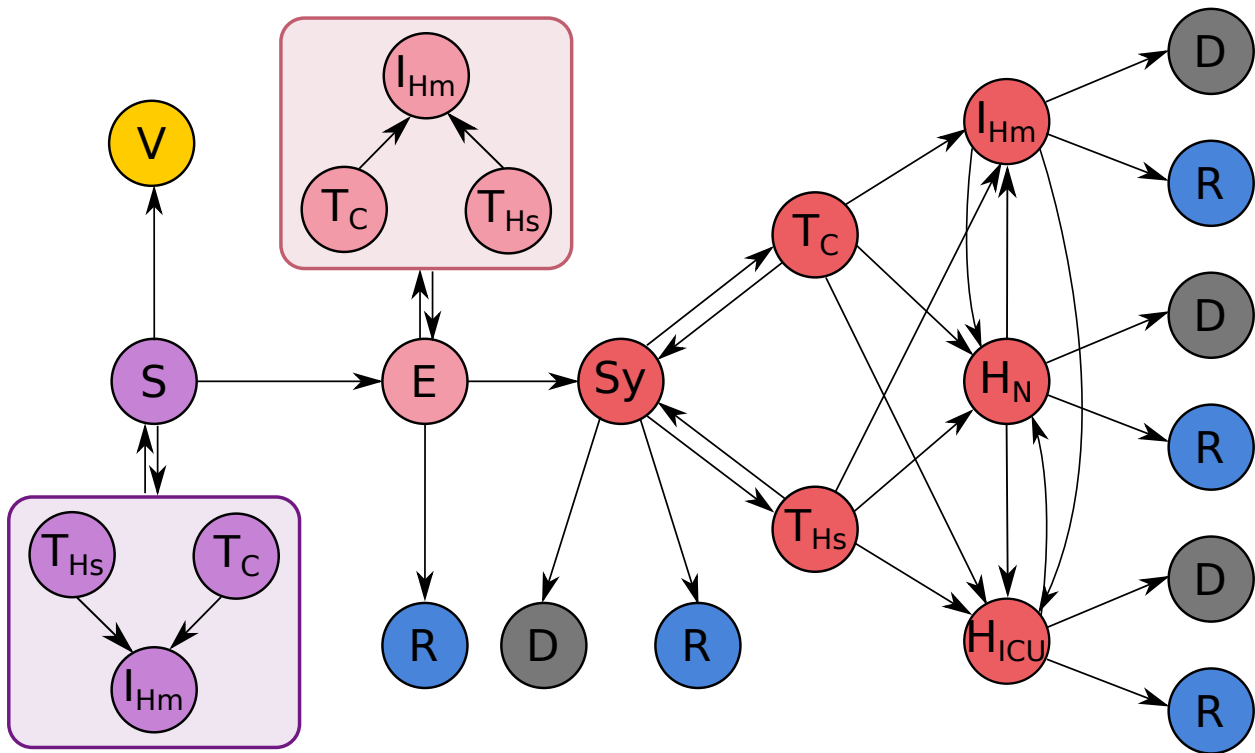


Figure 4: Schematic representation of modeled agent states and their possible transitions. Agent in the model could be in one of the following states: vaccinated (V); susceptible (S); exposed (E); symptomatic (Sy); removed-dead (D); removed-healthy/recovered (R). Agents in different states can undergo testing in a test car (T_C), or a hospital (T_{Hs}) after which they can be treated through home isolation (I_{Hm}), normal hospitalization (H_N), or hospitalization in an intensive care unit, ICU (H_{ICU}). In addition to symptomatic agents, exposed agents and agents who had COVID-19-like symptoms but were not COVID-19-infected (for example, because of the flu) could be tested.

316 in drive-through facilities (T_C), which were assumed not to carry the risk of infection. [45]
 317 All the agents who were waiting to be tested or were waiting for the results of a test were
 318 home-isolated. Hence, they could not visit any location. The result of a test could be false
 319 or true positive, or false or true negative.

320 Agents who tested positive (either true or false) were subject to three different treatment
 321 options: home isolation (I_{Hm}), normal hospitalization (H_N), and hospitalization in an in-
 322 tensive care unit, ICU (H_{ICU}). Exposed agents who tested positive were home-isolated un-
 323 til they became symptomatic. At that point, they could continue to be treated at home, or
 324 they could be hospitalized, changing their state to H_N or H_{ICU} . Symptomatic agents could
 325 undergo different treatment during the disease progression, eventually being removed from
 326 the model either as healthy/recovered (R) or dead (D). Removed agents did not contribute
 327 to the infection process. Untested symptomatic agents would not undergo any treatment,
 328 but they were eventually removed from the model, similar to the treated agents. However,
 329 untested agents who developed serious illness that would have required ICU had an in-
 330 creased probability of dying (D) with respect to those who received treatment.

331 Our model also includes confounding factors at testing sites introduced by individuals with
 332 influenza-like symptoms, similar to COVID-19, who required testing. [46] We relied on avail-
 333 able data from Centers for Disease Control and Prevention (CDC) to introduce a constant
 334 number of such individuals in the population, rather than coupling a co-morbidity flu and
 335 cold model to our COVID-19 model. These individuals tended to increase the burden on
 336 testing sites, and they were exposed to a higher risk of infection from COVID-19 when vis-
 337 iting the testing site. Finally, they might increase the number of false positives upon COVID-
 338 19 testing. Such agents were still susceptible to COVID-19.

339 The ABM utilizes a single parameter that captures the efficacy of testing practices with-
 340 out explicitly incorporating contact tracing practices at the individual level. This parame-
 341 ter determines the probability that an agent is tested, which is different depending on their
 342 health state (susceptible with influenza-like symptoms, exposed, and symptomatic agents).
 343 All the parameters that characterize the mechanisms described in the above are reported in
 344 the Supporting Information.

345 4.3 Human mobility

346 An agent who took public transportation was assigned the route that was most suitable for
 347 their workplace location. Best routes for each possible destination were approximated us-
 348 ing transit suggestions available from Google Maps. [33] The agents were grouped by routes,
 349 creating conditions for the disease spread. Carpools, on the other hand, were created only
 350 based on the workplace location and travel time of agents. Using the US Census data [30]
 351 on the number of passengers people commonly travel with, we maintained a realistic distri-
 352 bution of carpool capacities.

353 Agents who were not quarantined were allowed to perform non-essential activities, that is,
 354 to visit leisure locations or each other at their households. The same activity was imposed
 355 on all the agents in the same household. The assignment of a non-essential activity was ex-
 356 ecuted for each time-step for a predetermined fraction of households $\phi_N(t)$, who was chosen
 357 according to the extent of the reopening efforts as

$$\phi_N(t) = \min\{\underline{\phi}_N + \rho(\bar{\phi}_N - \underline{\phi}_N)t, \underline{\phi}_N\}, \quad (1)$$

where $\underline{\phi}_N$ and $\overline{\phi}_N$ are the minimum and maximum fraction of households that do non-essential activities, and ρ is the reopening rate, as detailed in the Supporting Information.

Households that were sampled to perform non-essential activities, were assigned either to a leisure location or to socially visit another household drawn uniformly at random. These two activities were assumed to be selected with equal probability. The leisure location itself was assigned by sampling a modified power-law distribution, shown to match mobility patterns of individuals, according to their cell phone records.^[47] Specifically, at each time-step, each household that was part of the predetermined fraction was assigned a leisure location ℓ , $d_{i\ell}$ km away from their home, with a probability $q_{i\ell}$, such that

$$q_{i\ell} \propto (d_{i\ell} + d_{r0})^{-\kappa_1} \exp\left(-\frac{d_{i\ell}}{\kappa_2}\right), \quad (2)$$

where $d_{r0} = 1.5$ km, $\kappa_1 = 1.75$, and $\kappa_2 = 400$ from Gonzalez *et al.*^[47]

The current reopening rate in the town was estimated based on mobility data from Safegraph.^[34] Specifically, data representing number of visits to individual points-of-interest by day, normalized, and smoothed with a seven-day window was extracted for the New York/New Jersey region for a period of three months starting from January 17, 2021. A straight line fit to this data revealed a reopening rate of 0.28%/day.

4.4 COVID-19 transmission

A susceptible (S) agent i could become infected with COVID-19 (and thus exposed, E) at time t with the probability

$$p_i(t) := 1 - e^{-\Delta t \Lambda_i(t)}, \quad (3)$$

where $\Delta t = 0.25$ day is the duration of a time-step and $\Lambda_i(t)$ reflects the infectiousness of all the locations that the agent is associated with. Specifically, $\Lambda_i(t)$ included contributions from different location types associated with agent i as,

$$\begin{aligned} \Lambda_i(t) := & \lambda_{Hh, f_{Hh}(i)}(t) + \lambda_{W, f_W(i)}(t) + \lambda_{Sc, f_{Sc}(i)}(t) + \lambda_{Rh, f_{Rh}(i)}(t) \\ & + \lambda_{Hsp, f_{Hsp}(i)}(t) + \lambda_{Tr, f_{Tr}(i)}(t) + \lambda_{N, f_N(i,t)}(t), \end{aligned} \quad (4)$$

where $\lambda_{\bullet, \ell}(t)$ represents the infectiousness of location ℓ at time t (the first subscript is used to denote the type of location: Hh for households, W for workplaces, Sc for schools, Rh for retirement homes, Hsp for hospital, Tr for public transit and carpooling, and N for non-essential activity) and function $f_{\bullet}(i)$ selects the location type that agent i is assigned to. Note that the assignment of agents to non-essential activity was generally time-varying, since agents might visit different venues at different times.

The infectiousness of each in-town location (excluding non-essential activity) was proportional to the fraction of infectious agents (exposed and symptomatic individuals) at that location and to a characteristic transmission rate β_{\bullet} , which varied across the different types of locations, accounting for their varying risk. Precise expressions for the infectiousness of each type of location are reported in the Supporting Information. For out-of-town workplaces, infectiousness was assumed to be proportional to the estimated fraction of infected individuals in the neighboring US region^[48–50] and to the transmission rate associated with workplaces, as detailed in the Supporting Information.

While the infectiousness at private gatherings was modeled using the household transmission rate (see Supporting Information), the infectiousness at a leisure location was proportional to the fraction of infectious individuals in that location and to the transmission rate associated with it. We assumed that the transmission rate β_L was time-varying, increasing with reopening efforts. Specifically, we set the full-capacity transmission rate of leisure locations, $\bar{\beta}_L$, using data on average secondary-attack-rates from real-life COVID-19 outbreaks reported by Koh *et al.* [51] Then, we set the initial transmission rate as 57% of such a quantity, that is, $\underline{\beta}_L = 0.57\bar{\beta}_L$, based on Google Mobility Reports. [52] Hence, the transmission rate in leisure locations would at the reopening rate ρ according to

$$\beta_L(t) = \min\{\underline{\beta}_L + \rho(\bar{\beta}_L - \underline{\beta}_L)t, \bar{\beta}_L\}, \quad (5)$$

where $t = 0$ is the start of the simulation, details can be found in the Supporting Information.

4.5 Model calibration

The backbone of the ABM is based on the work of Truszkowska *et al.*, [28] where calibration was performed on the officially reported data on the COVID-19 epidemic in New Rochelle, NY during the first wave of COVID-19 (March through July of 2020). [53] The calibration parameters were limited to only eight unknown variables, namely, number of initially infected agents, time-varying fraction of exposed and symptomatic agents who were tested, transmission reductions associated with the lockdown and three local reopening phases, and age-distribution of asymptomatic agents. All other model parameters obtained from established sources, including clinical data on COVID-19. Through this effort, we identified a base parameter set that allowed us to closely replicate the evolution of the first wave of COVID-19 in the town. Specifically, we matched the total number of detected cases, the number of new cases confirmed every week, the weekly average of individuals treated for COVID-19, and the number of casualties reported each week.

Aiming to achieve conditions as close as possible to the current ones, we updated the original set with more recent data and estimates on closures and testing practices. To acknowledge the fact that businesses are now open but not operating at full capacity, we scaled down the infection risk in all the general workplaces using the Google COVID-19 Mobility Report for Westchester county. [52] Likewise, since schools are now operating in a hybrid mode, [54] we reduced transmission rates accordingly. The complete list of parameters and their sources are available in the Supporting Information.

Different testing levels for simulating the different scenarios were implemented by increasing the probability of testing for an asymptomatic and symptomatic agent during the simulation. For example, for perfect testing all asymptomatic and symptomatic agents were tested, whereas for low testing a symptomatic agent was tested with a probability of 0.64 and an asymptomatic agent was tested with a probability of 0.44.

Supporting information

Supporting Information is available from the Wiley Online Library or the corresponding author. The database and the simulation code are available at <https://github.com/Dynamical-Systems-Laboratory/NR-population-mobility> and <https://github.com/Dynamical-Systems-Laboratory/ABM-COVID-Mobility>, respectively.

Author contributions

Conceptualization—AT, SB, ZPJ, AR, MP; methodology—AT, SB; software—AT, SB; validation—AT; investigation—all the authors; resources—MP; data curation—AT, MT; writing—original draft preparation—AT, LZ, SB, AR, MP; writing—review and editing—MT, EC, ZPJ; visualization—AT; supervision—SB, EC, ZPJ, AR, MP; project administration—MP; funding acquisition—SB, ZPJ, AR, MP.

Acknowledgements

This work was partially supported by National Science Foundation (CMMI-1561134, CMMI-2027990, and CMMI-2027988) and by Compagnia di San Paolo.

Conflict of interest

The authors declare no conflict of interest.

References

- [1] Our World in Data, Coronavirus (COVID-19) Vaccinations, <https://ourworldindata.org/covid-vaccinations>, (Accessed: June 2021).
- [2] Forbes, <https://www.forbes.com/advisor/personal-finance/americans-still-split-about-reopening-economy>, (Accessed: June 2021).
- [3] Pew Research, A year of U.S. public opinion on the coronavirus pandemic, <https://www.pewresearch.org/2021/03/05/a-year-of-u-s-public-opinion-on-the-coronavirus-pandemic>, (Accessed: June 2021).
- [4] New York Times, New York's reopening is 'wild,' 'hopeful,' 'exciting,' and 'bad', <https://www.nytimes.com/2021/03/25/opinion/new-york-reopening-bars.html>, (Accessed: June 2021).
- [5] E. Estrada, *Phys. Rep.* **2020**, *869*, 1.
- [6] A. Vespignani, H. Tian, C. Dye, J. O. Lloyd-Smith, R. M. Eggo, M. Shrestha, S. V. Scarpino, B. Gutierrez, M. U. G. Kraemer, J. Wu, K. Leung, G. M. Leung, *Nat. Rev. Phys.* **2020**, *2*, 279.
- [7] A. L. Bertozzi, E. Franco, G. Mohler, M. B. Short, D. Sledge, *Proc. Natl. Acad. Sci. USA* **2020**, *117*, 29, 16732.
- [8] N. Perra, *Phys. Rep.* **2021**, in press.
- [9] F. Della Rossa, D. Salzano, A. Di Meglio, F. De Lellis, M. Coraggio, C. Calabrese, A. Guarino, R. Cardona-Rivera, P. De Lellis, D. Liuzza, F. Lo Iudice, G. Russo, M. di Bernardo, *Nat. Comm.* **2020**, *11*, 1, 5106.
- [10] F. Pinotti, L. Di Domenico, E. Ortega, M. Mancastroppa, G. Pullano, E. Valdano, P.-Y. Boëlle, C. Poletto, V. Colizza, *PLOS Med.* **2020**, *17*, 7, 1.
- [11] A. Arenas, W. Cota, J. Gómez-Gardeñes, S. Gómez, C. Granell, J. T. Matamalas, D. Soriano-Paños, B. Steinegger, *Phys. Rev. X* **2020**, *10*, 041055.
- [12] F. Parino, L. Zino, M. Porfiri, A. Rizzo, *J. R. Soc. Interface* **2021**, *18*, 175, 20200875.

- 471 [13] K. H. Cheong, T. Wen, J. W. Lai, *Adv. Sci.* **2020**, 7, 24, 2002324.
- 472 [14] U. Goldsztejn, D. Schwartzman, A. Nehorai, *PLOS One* **2020**, 15, 12, 1.
- 473 [15] H. Noorbhai, *Ann. Med. Surg.* **2020**, 57, 5.
- 474 [16] K. M. Bubar, K. Reinholt, S. M. Kissler, M. Lipsitch, S. Cobey, Y. H. Grad, D. B.
475 Larremore, *Science* **2021**, 371, 6532, 916.
- 476 [17] P. C. Jentsch, M. Anand, C. T. Bauch, *Lancet Infect. Dis.* **2021**, in press.
- 477 [18] M. Shen, J. Zu, C. K. Fairley, J. A. Pagán, L. An, Z. Du, Y. Guo, L. Rong, Y. Xiao,
478 G. Zhuang, Y. Li, L. Zhang, *Vaccine* **2021**, 39, 16, 2295.
- 479 [19] G. Giordano, M. Colaneri, A. D. Filippo, F. Blanchini, P. Bolzern, G. D. Nicolao,
480 P. Sacchi, R. Bruno, P. Colaneri, *Nat. Med.* **2021**, in press.
- 481 [20] S. Moore, E. M. Hill, M. J. Tildesley, L. Dyson, M. J. Keeling, *Lancet Infect. Dis.*
482 **2021**, in press.
- 483 [21] S. Grundel, S. Heyder, T. Hotz, T. K. S. Ritschel, P. Sauerteig, K. Worthmann,
484 *Preprint at medRxiv ht tp s : // do i . org / 10 . 1 1 0 1 / 2 0 2 0 . 1 2 . 2 2 . 2 0 2 4 8 7 0 7*
485 **2020**.
- 486 [22] M. Galanti, S. Pei, T. K. Yamana, F. J. Angulo, A. Charos, D. L. Swerdlow,
487 J. Shaman, *Preprint at medRxiv ht tp s : // do i . org / 10 . 1 1 0 1 / 2 0 2 0 . 1 2 . 2 3*
488 *. 2 0 2 4 8 7 8 4* **2020**.
- 489 [23] N. Agarwal, A. Komo, C. A. Patel, P. A. Pathak, U. Unver, *Preprint at EconPapers*
490 *ht tp s : // Ec on Pa p e r s . r e p e c . o r g / R e P E C : n b r : n b e r w o : 2 8 5 1 9* **2021**.
- 491 [24] A. N. Kraay, M. E. Gallagher, Y. Ge, P. Han, J. M. Baker, K. Koelle, A. Handel,
492 B. A. Lopman, *Preprint at medRxiv ht tp s : // do i . org / 10 . 1 1 0 1 / 2 0 2 1 . 0 3 .*
493 *1 2 . 2 1 2 5 3 4 8 1* **2021**.
- 494 [25] N. M. Ferguson, D. Laydon, G. Nedjati-Gilani, N. Imai, K. Ainslie, S. B.
495 Marc Baguelin, A. Boonyasiri, Z. Cucunubá, G. Cuomo-Dannenburg, A. Dighe,
496 I. Dorigatti, H. Fu, K. Gaythorpe, W. Green, A. Hamlet, W. Hinsley, L. C. Okell,
497 S. van Elsland, H. Thompson, R. Verity, E. Volz, H. Wang, Y. Wang, C. W. Patrick
498 GT Walker, P. Winskill, C. Whittaker, C. A. Donnelly, S. Riley, A. C. Ghani, Impact
499 of non-pharmaceutical interventions (NPIs) to reduce COVID-19 mortality and health-
500 care demand, Report of the Imperial College London, UK [https://doi.org/10.255](https://doi.org/10.25561/77482)
501 [61/77482](https://doi.org/10.25561/77482), (Accessed: June 2021).
- 502 [26] M. Chinazzi, J. T. Davis, M. Ajelli, C. Gioannini, M. Litvinova, S. Merler, A. P. y Pi-
503 ontti, K. Mu, L. Rossi, K. Sun, C. Viboud, X. Xiong, H. Yu, M. E. Halloran, I. M.
504 Longini, A. Vespignani, *Science* **2020**, 368, 6489, 395.
- 505 [27] N. Hoertel, M. Blachier, C. Blanco, M. Olfson, M. Massetti, M. S. Rico, F. Limosin,
506 H. Leleu, *Nat. Med.* **2020**, 26, 9, 1417.
- 507 [28] A. Truszkowska, B. Behring, J. Hasanyan, L. Zino, S. Butail, E. Caroppo, Z.-P. Jiang,
508 A. Rizzo, M. Porfiri, *Adv. Theory Simul.* **2021**, 4, 3, 2170005.

- 509 [29] CNN News, New York officials traced more than 50 coronavirus cases back to one at-
510 torney, [https://www.cnn.com/2020/03/11/us/new-rochelle-attorney-containm
ent-area/index.html](https://www.cnn.com/2020/03/11/us/new-rochelle-attorney-containm
511 ent-area/index.html), (Accessed: June 2021).
- 512 [30] United States Census Bureau, Explore Census Data, [https://data.census.gov/ce
dsci](https://data.census.gov/ce
513 dsci), (Accessed: June 2021).
- 514 [31] United States Census Bureau, America: a nation of small towns, [https://www.cens
516 us.gov/library/stories/2020/05/america-a-nation-of-small-towns.html](https://www.cens
515 us.gov/library/stories/2020/05/america-a-nation-of-small-towns.html),
(Accessed: June 2021).
- 517 [32] OpenStreetMap Community, Openstreetmap, <https://www.openstreetmap.org>,
518 **2021**, (Accessed: June 2021).
- 519 [33] Google, Google Maps, <https://www.google.com/maps>, **2021**, (Accessed: June 2021).
- 520 [34] SafeGraph Inc., SafeGraph, <https://www.safegraph.com>, (Accessed: June 2021).
- 521 [35] G. Young, P. Xiao, K. Newcomb, E. Michael, *preprint at arXiv ht tps://arxiv.org/ab s/2103.06120* **2021**.
- 522
- 523 [36] Healthline, Vaccinated or not, COVID-19 testing is still important, here's why, [https:
//www.healthline.com/health-news/vaccinated-or-not-covid-19-testing-is-s
till-important-heres-why#Fewer-cases,-less-testing](https:
524 //www.healthline.com/health-news/vaccinated-or-not-covid-19-testing-is-s
525 till-important-heres-why#Fewer-cases,-less-testing), (Accessed: June 2021).
- 526 [37] Scientific American, Safely reopening requires testing, tracing and isolation, not just
527 vaccines, [https://www.scientificamerican.com/article/safely-reopening-re
529 quires-testing-tracing-and-isolation-not-just-vaccines](https://www.scientificamerican.com/article/safely-reopening-re
528 quires-testing-tracing-and-isolation-not-just-vaccines), (Accessed: June
2021).
- 530 [38] UK Government, New campaign urges public to get tested twice a week, [https://ww
w.gov.uk/government/news/new-campaign-urges-public-to-get-tested-twice-a
-week](https://ww
531 w.gov.uk/government/news/new-campaign-urges-public-to-get-tested-twice-a
532 -week), (Accessed: June 2021).
- 533 [39] A. Pastore y Piontti, N. Perra, L. Rossi, N. Samay, A. Vespignani, *Charting the Next
534 Pandemic*, Springer International Publishing, Cham, Switzerland, **2019**.
- 535 [40] A. Reyna-Lara, D. Soriano-Paños, S. Gómez, C. Granell, J. T. Matamalas, B. Steineg-
536 ger, A. Arenas, J. Gómez-Gardeñes, *Physical Review Research* **2021**, *3*, 1, 013163.
- 537 [41] S. Kojaku, L. Hébert-Dufresne, E. Mones, S. Lehmann, Y.-Y. Ahn, *Nature Physics*
538 **2021**, *17*, 5, 652.
- 539 [42] Institute for Education Science, National Center for Education Statistics, [https:
//nces.ed.gov](https:
540 //nces.ed.gov), (Accessed: June 2021).
- 541 [43] New York State Department of Health, NYS Health Profiles — Montefiore New
542 Rochelle Hospital, <https://profiles.health.ny.gov/hospital/view/103001>,
543 (Accessed: June 2021).
- 544 [44] American Hospital Directory, Montefiore New Rochelle Hospital, [https://www.ahd.
com/free_profile/330184/Montefiore_New_Rochelle_Hospital/New_Rochelle/Ne
w_York](https://www.ahd.
545 com/free_profile/330184/Montefiore_New_Rochelle_Hospital/New_Rochelle/Ne
546 w_York), (Accessed: June 2021).

- 547 [45] A. Shah, D. Challener, A. J. Tande, M. Mahmood, J. C. O'Horo, E. Berbari, S. J.
548 Crane, *Mayo Clin. Proc.* **2020**, *95*, 1420.
- 549 [46] Centers for Disease Control and Prevention, Similarities and differences between flu
550 and COVID-19, <https://www.cdc.gov/flu/symptoms/flu-vs-covid19.htm>,
551 (Accessed: June 2021).
- 552 [47] M. C. Gonzalez, C. A. Hidalgo, A.-L. Barabasi, *Nature* **2008**, *453*, 7196, 779.
- 553 [48] COVID-19 Forecast Hub, COVID-19 Connecticut weekly forecast summary, https://covid19forecasthub.org/reports/single_page.html?state=CT&week=2021-03-30#County_level, (Accessed: June 2021).
554
555
- 556 [49] COVID-19 Forecast Hub, COVID-19 New York weekly forecast summary, https://covid19forecasthub.org/reports/single_page.html?state=NY&week=2021-03-30#County_level, (Accessed: June 2021).
557
558
- 559 [50] United States Census Bureau, QuickFacts, Westchester County, New York; United
560 States, <https://www.census.gov/quickfacts/fact/table/westchestercountynework,US/PST045219>, (Accessed: June 2021).
561
- 562 [51] W. C. Koh, L. Naing, L. Chaw, M. A. Rosledzana, M. F. Alikhan, S. A. Jamaludin,
563 F. Amin, A. Omar, A. Shazli, M. Griffith, et al., *PLOS One* **2020**, *15*, 10, e0240205.
- 564 [52] Google, COVID-19 Community Mobility Report for New York state counties, March
565 31st 2021, https://www.gstatic.com/covid19/mobility/2021-03-31_US_New_York_Mobility_Report_en.pdf, (Accessed: June 2021).
566
- 567 [53] Westchester County, Westchester County official Twitter account, <https://twitter.com/westchestergov>, **2021**.
568
- 569 [54] City School District of New Rochelle, COVID Resource Center, https://www.nred.org/covid_resource_center#gsc.tab=0, (Accessed: June 2021).
570

